SCIENTIFIC REPORTS

OPEN

SUBJECT AREAS:
ELECTRONIC DEVICES
QUANTUM INFORMATION
OPTICAL MATERIALS AND STRUCTURES
NANOPHOTONICS AND PLASMONICS

Received
7 January 2013

Accepted
9 April 2013

Published
24 April 2013

Correspondence and requests for materials should be addressed to J.M.A. (jmalbella@icmm.csic.es)

Exciton and core-level electron confinement effects in transparent ZnO thin films

Adolfo A. Mosquera[1], David Horwat[2], Alexandr Rashkovskiy[4], Anatoly Kovalev[4], Patrice Miska[3], Dmitry Wainstein[4], Jose M. Albella[1] & Jose L. Endrino[5]

[1]Instituto de Ciencia de Materiales de Madrid, Consejo Superior de Investigaciones Científicas, E-28049 Madrid, Spain, [2]Institut Jean Lamour, Université de Lorraine, UMR 7198, Nancy, F-54000, France, [3]CNRS, Institut Jean Lamour, UMR 7198, Nancy, F-54000, France, [4]Surface Phenomena Researches Group, 2nd Baumanskaya str. 9/23, CNIICHERMET, off. 475, 105005 Moscow, Russia, [5]Abengoa Research S.L., C/ Energía Solar 1, Palmas Altas 41014, Sevilla, Spain.

The excitonic light emission of ZnO films have been investigated by means of photoluminescence measurements in ultraviolet-visible region. Exciton confinement effects have been observed in thin ZnO coatings with thickness below 20 nm. This is enhanced by a rise of the intensity and a blue shift of the photoluminescence peak after extraction of the adsorbed species upon annealing in air. It is found experimentally that the free exciton energy (determined by the photoluminescence peak) is inversely proportional to the square of the thickness while core-level binding energy is inversely proportional to the thickness. These findings correlate very well with the theory of kinetic and potential confinements.

In the last decades zinc oxide has been widely investigated in different industrial areas such as opto-and nano-electronics[1,2], rubber industry, paints, ceramics and in the pharmaceutical industry. In these applications the special characteristics of ZnO-based compounds allow them to be used as a transparent conductor or semiconductor material. This is why new technological challenges in the electronic industry make ZnO a unique material for improving and fabricating novel products. Specifically, ZnO has been widely investigated in applications such as automobile devices (e.g. panel lighting), traffic lights, optical recording media, scanning readers, video game consoles and LEDs[3]. In addition, UV LEDs sources based on ZnO are being applied in UV curing, counterfeit detection, and medical instrumentation[4], due to its outstanding properties, i.e. a wide band gap (3.37 eV), high absorption in the UV range and higher excitonic binding energy (60 meV)[5] than other materials, with similar applications such as GaN (28 meV)[6].

Nowadays, ZnO research in the optoelectronics field is growing and it is focused on improving the ZnO exciton emission in the blue-UV region, taking advantage of its high exciton binding energy and efficient radiative recombination even at room temperature[7,8]. Photoluminescence (PL) in the UV region is caused by free electron-hole recombination phenomena in the near band edge. In the visible region, PL is due to the presence of chemical and structural defects such as oxygen and zinc vacancies, and oxygen and zinc interstitials[9]. Free excitons are bound electron-hole pairs that can move together through the crystal[10] and are useful in photovoltaic, optoelectronics[11,12] and solar cell devices[13], while excitons bound to structural defects in the material, can be used as laser media[14,15].

In this work, ZnO thin films, of hexagonal wurtzite structure and with the preferential growth along the <0002> direction, have been deposited by DC magnetron sputtering[16,17] on glass substrates. Optical transmittance and PL spectra were used to study the exciton response as a function of film thickness. Different works have shown a dependence of the exciton energy on the dimension of ZnO nano-objects, mostly based on theoretical research or experimental measurements on ZnO quantum dots[18–20]. One of these reports indicates confinement effects in polycrystalline ZnO films with the grain size as the confined dimension[21]. In this study we investigate on the dependence of the electron core levels energy, and free excitons optical emission energy on the thickness of the ZnO thin films.

Results

ZnO films were deposited onto glass substrates in order to characterize the morphology parameters and crystallography by X-ray diffraction (XRD) and profilometry techniques. The experiments were carried out for

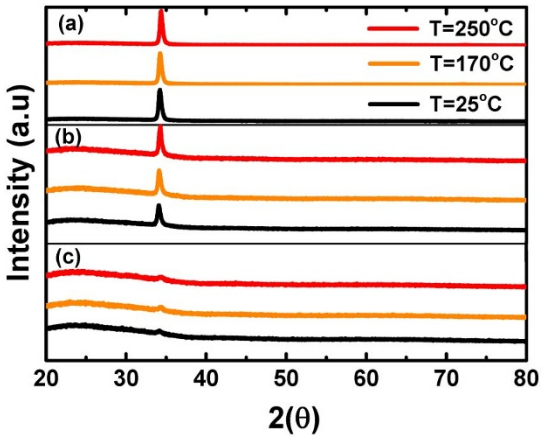

Figure 1 | XRD (theta-2 theta scan) diffractograms of the ZnO thin films with different thicknesses (a) 116.0 nm, (b) 51.5 nm and (c) 20.4 nm, without annealing and after annealing at 170 and 250°C for 1 hour.

as-deposited and annealed films. The annealing treatment during 1 hour was applied in order to improve the film crystallinity as well as to clean the surface from adsorbed impurities. Figure 1 shows the XRD patterns for the as-deposited samples as well as films annealed at 170°C and 250°C during 1 hour. The ZnO films with thickness above 20 nm show hexagonal structure with a single (0002) peak, implying that the ZnO films exhibit a preferred c-axis orientation perpendicular to the surface. As the annealing temperature was increased the intensity of the XRD peak also increased, indicating an enhanced crystallinity.

The electronic structure is known to be a property for compounds with a given chemical composition. For pure ionic compounds, the binding energy of core-level electrons should be the same as for free-ions (i.e. Zn^{2+} and O^{2-}), but shifted to higher energies for donor, and to lower energies for acceptor levels. As previously shown[22], there could be another shift of core-level energies to higher binding energies when the grain size decreases to nanoscale giving rise to quantum confinement effects. In Figure 2, showing the XPS spectra of ZnO thin films with different thickness, it is clearly appreciated that, besides the strong chemical shift in binding energies, there is an additional force that pulls the core-level electrons to higher energies as compared to the standard bulk material (1022.0 eV and 1045.0 eV for Zn2p level, and 532.0 eV for 01s level). The shift in binding energies can reach values up to +2.0 eV in the case of 10.0 nm thick ZnO films.

In the O1s spectra of samples without Ar^+ ion beam etching (see methods), Figure 2b (subplot), the peak can be decomposed in two main peaks located between 531.5–532.5 eV attributed to OH species[23]. After etching for 10 min of the ZnO films, the OH radicals disappear and only one peak, corresponding to O-Zn bonds located at ~530.5 eV, was observed[24].

Figure 3 shows AFM images for samples with two different thicknesses. The ZnO film with t = 10.0 nm (Figure 3a) shows an island structure, which is likely determined by the glass substrate[25], whereas the films with thickness t = 116.0 nm have a homogeneous surface with a compact structure. The AFM images, Figure 3b and 3c, reveal that the ZnO films with t = 116.0 nm have close packed nanograins with mean grain size of 30.1 ± 1.3 nm. The grain size was determined using GWYDDION software on Figure 3 and was similar to the grain size determined by XRD, as shown in table 1. The surface roughness of these ZnO films was found to be between 2.3 and 19.2 nm.

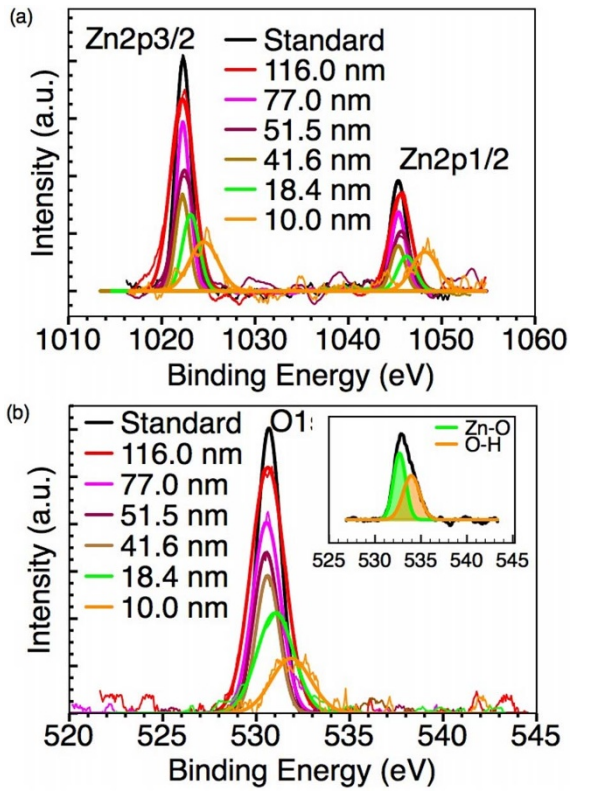

Figure 2 | Core-level Zn2p (a) and O1s (b) spectra of ZnO films of different thicknesses after and before (subplot) Ar^+ ions etching.

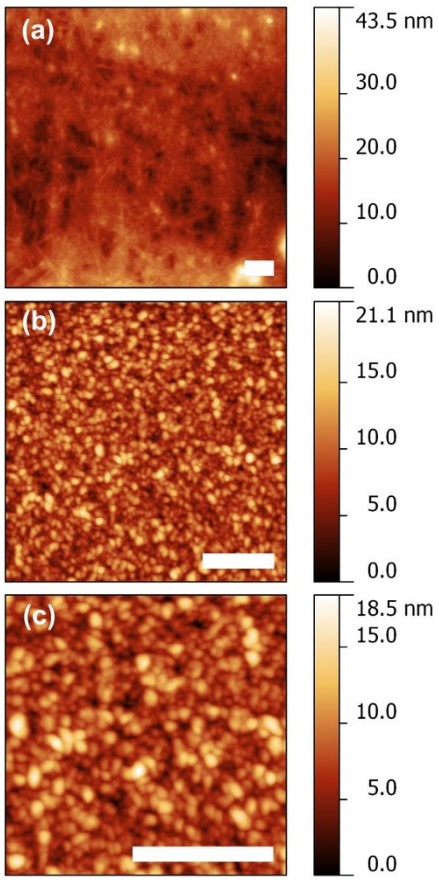

Figure 3 | AFM images of the as-grown ZnO thin films with different thickness (a) t = 10.0 nm and (b), (c) t = 116.0 nm. Note the different magnification (white scale line = 500 nm).

Table 1 | Main characteristics of ZnO films

Thickness (±1.3 nm)	Roughness (±0.6 nm)	Grain size *g* (nm)	
	Profilometry	XRD	
		25°C	250°C
10.0	—	—	—
18.4	2.3	14.6	16.8
20.4	5.4	14.6	15.9
41.6	9.2	24.6	25.7
51.5	4.9	25.8	26.2
116.0	4.9	27.6	28.2

Figure 4a shows Zn-L_3 XANES spectra of the ZnO films. In this case, as 3d states are occupied in ZnO, the Zn-L_3 edge is very sensitive to transitions from 2p electrons to both 4s and 4d unoccupied states. Features from A to D are located at 1015.5, 1019.0, 1022.2 and 1024.5 eV respectively, and are very similar to those reported in the literature for ZnO films of wurtzite crystal structure[26]. Feature A corresponds to Zn 4s derived state, while features B, C and D correspond to Zn 4d derived states. Figure 4b, shows the normalized total electron yield (TEYN) and total fluorescence yield (TFYN) of the O-K XANES spectra. This edge gives information about 1s to 2p transitions. Six different features from A to F were located at 534.3, 538.7, 542.3, 544.5, 550.9 and 556.8 eV, respectively. For the thickest films (above 50 nm) the TEYN and TFYN spectra are rather similar for all of them. These features are also more localized if they are compared with the thinnest film (t = 20.4 nm). Moreover, feature A is more peaked in the TEYN spectra indicating that it is more sensitive to surface states. Feature A has been proposed to be associated to σ-type interaction between Zn and O planes[27]. Modification of its intensity and energy can be related to surface relaxation phenomena. In contrast, the spectra corresponding to the film of lowest thickness exhibit increased and decreased intensity of the B and A contribution with reference to the thickest films, respectively. The high amplitude of feature B indicates the surface is (0001) O-terminated[27,28]. The much weaker amplitude of feature A indicates a lower hybridization of Zn and O atoms. It is worth noting that ultrathin ZnO films present an amorphous organization in the first few nanometers that can serve as a support for the growth of few monolayers of graphitic-like ZnO itself facilitating the development the self-textured c-axis oriented wurtzite ZnO film[29]. Indeed, the electronic structure is sensitive to the films thickness, and the sensitivity is more pronounced for the thinnest films, which is likely due to a distortion of the local bonds with reference to thickest films.

The transmittance spectra of the ZnO films are illustrated in Figure 5. All the films show a high optical transmittance, around 90%, in the visible region. This is usually associated to the absence of, or minute presence of, oxygen vacancies in the films. In other words, the films composition is close to stoichiometric ZnO[28]. When the temperature was increased to 170°C the optical transmittance increased slightly. Further heating to 250°C produced a decrease in optical transmittance. We can attribute this evolution to a change in the local chemistry upon annealing. The evolution at 170°C is correlated to the removal of adsorbed species evidenced by XPS.

Room temperature PL emission spectra of the films before and after annealing at 170°C are shown in Figure 6. As-deposited samples exhibit complex PL spectra with several bands, covering the UV and visible ranges. It is generally admitted that the signal in the visible range arises from excitons that are bound to acceptor and donor defects (bound excitons)[30,31]. After annealing at 170°C during 1 hour, the signal weakens significantly in the visible range whereas a new peak develops in the UV region. This peak has been ascribed to the free exciton emission, also referred as near band edge emission. This exciton peak was located around 379 nm in the thinnest film and shifts to higher wavelengths as the thickness increases (see Figure 6d). Only the thickest film showed a clear exciton response before annealing. The shift observed in the PL energy cannot be associated to the Burstein-Moss[32,33] effect since this effect is only observed in highly doped ZnO films[34,35]. Moreover, all films have been prepared with different thickness under the same reactive conditions, i.e. constant flux of Zn and O atoms condensing to form the ZnO films. In addition, there are no reports of Burstein-Moss effect on the room temperature PL measurements of undoped ZnO films, where the free exciton emission is dominant[36,37]

By plotting the shift in the free exciton energy as a function of thickness (Figure 7), it is observed a shift towards higher energies in a monotonous way as the film thickness decreases. For the thinnest deposited ZnO film, the UV emission peak was located at 3.56 eV with a shift of 0.36 eV from the exciton emission peak of thickest film, located at 3.20 eV. In addition, the core-level electron shift (deduced from XPS values of Figure 2) as a function of thickness is also shown in Figure 7. It reaches 2 eV for the thinnest film. A power function was used to fit both the core-level electron and free exciton shifts, showing a 1/t and $1/t^2$ thickness (t) dependence, respectively.

Discussion

The preferential growth plane observed in this work, along <0002> direction of the wurtzite structure, is related with the high texturization present in all the samples and is in line with previous reports[38]. When the temperature was increased no other diffraction peaks were

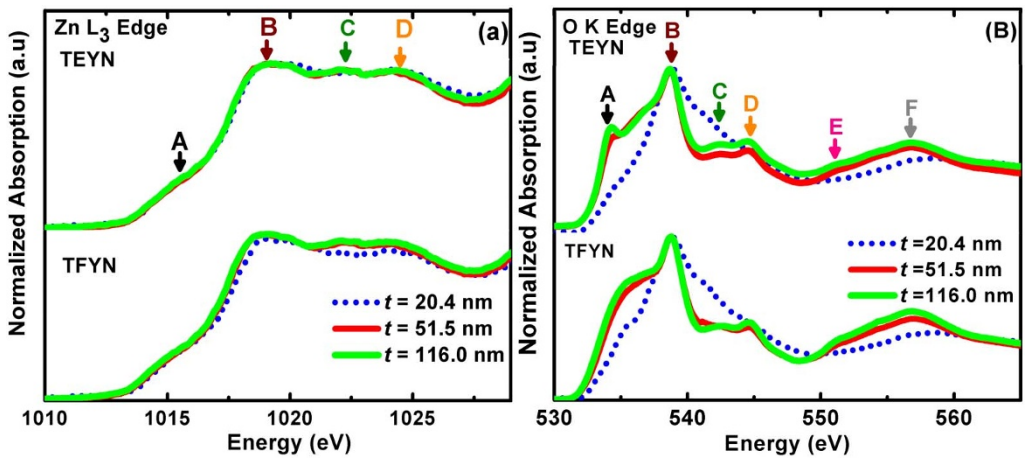

Figure 4 | TEYN and TFYN of the (a) Zn-L3 and (b) O-K edge XANES of the as-deposited ZnO thin films with different thickness (t).

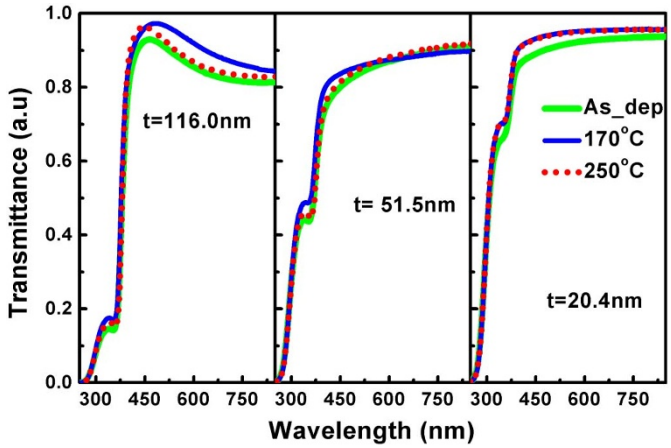

Figure 5 | Optical transmittance spectra of ZnO films with different thickness without and after annealing at 170°C and 250°C.

observed in the films and the magnitude of the peak was increased. The grain size of the ZnO films slightly increased with the temperature as reported in table 1 but this is not significant if the error of measurement is considered. It was impossible to correlate the shift in the core-level and free excitons emission energies with the grain size. In the as-deposited films, the peak was located at $2\theta = 34.0^{\circ}$, i.e. slightly below that found for ZnO powder (34.5°), revealing that the films may exhibit in-plane compressive stresses[39]. Not only the stress may affect the peak position but the presence of absorbed species. As it is well known, ZnO is a polar compound that can produce polar films[40-42], which easily adsorb radical species. When the annealing at 170°C was performed, these species have been released promoting the contraction of the unit cell and shift of the peak position to 34.4°. ZnO films as deposited or annealed at lower temperatures presented a high texturization but the crystal quality and chemistry were not suited to obtain a strong PL emission in the UV range.

According to the XPS analysis of results before annealing, reported in supplementary table S1, the surface of as-deposited ZnO films showed a low Zn/O ratio, with carbon concentration above 60 at%. These results clearly underline that the polarity of ZnO makes the films sensitive to ambient contaminant such as CO_2 and do not reveal the real composition of the films. The XPS spectra support this polarity effect of the surface of the films, since adsorbed OH species were identified from the O1s spectrum. Likewise, these species can also affect the optical and photoluminescence properties of the films. Nevertheless, the doublet lines of Zn observed in the XPS spectra confirm that most of Zn atoms remain in the films with a valence state of Zn^{2+} [43].

According to XANES spectra, for the thickest films (features B, C and D) there is no difference in the Zn L_3 edge, indicating that the electronic structure of these samples is very similar. However, for the thinnest films, B-D features do show a shift, and the intensity of the density of Zn4d states is lower than in the thickest films. Therefore, a different bonding state in the thinnest films occurs. In the O-K edge, the B-F features are very similar for all the thicker films, but feature A has a narrow peak in the TEYN spectra, thus indicating that it is sensitive to the surface states of these films. In addition, the spectrum of the thinnest film does not coincide with the spectra of the thickest films, and only feature B appears in the TEYN and TFYN spectra representing the unoccupied states at the very bottom of the conduction band, while for the thickest film the bottom level is represented by feature A. Hence, this difference could be interpreted as a variation in the band gap of the films.

In the PL spectra, ultraviolet and visible emission bands have been observed. Before annealing, the strong broad band in the visible region is related to defects present in ZnO, such as oxygen vacancies, interstitial zinc or zinc vacancies[44-46], that could be identified from PL measurement at low temperature, i.e. down to 10 K[47,48]. In the UV region, there was no clear exciton emission before annealing the ZnO films, likely due to the presence of a large amount of OH species on the surface of ZnO films as evidenced by XPS. The free exciton emission is known to be suppressed in the presence of these adsorbed species[49] and annealing the films at 170°C releases these species. It is observed that the intensity of the free exciton peak for the film with t = 116 nm is stronger than that of the thinnest film, with t = 20.4 nm. This is probably due to the fact that the volume unaffected by the presence of OH species is larger for the thicker film. Therefore, the surface condition is an important factor to interpret the UV optical properties since it may cover up the real free exciton emission. Moreover, as can be appreciated in Figure 7, the free exciton emission peak shifts to lower energies when the ZnO film thickness increases. Thus, for the thinnest ZnO film, the UV emission peak was shifted up by 0.36 eV from that observed at 3.20 eV for the thickest sample. Actually, the shift of the exciton peaks follows an inverse power law of the type $1/t^2$, which means that excitons are thickness-sensitive quasi-particles. More precisely, these are sensitive to geometrical constraints along the c-axis of the wurtzite cell

On the other hand, it has been observed that the core-level energy of the electrons also "feels" the thickness effect (see XPS spectra in Fig. 2). By plotting the dependence of average (Zn2p and O1s) core-

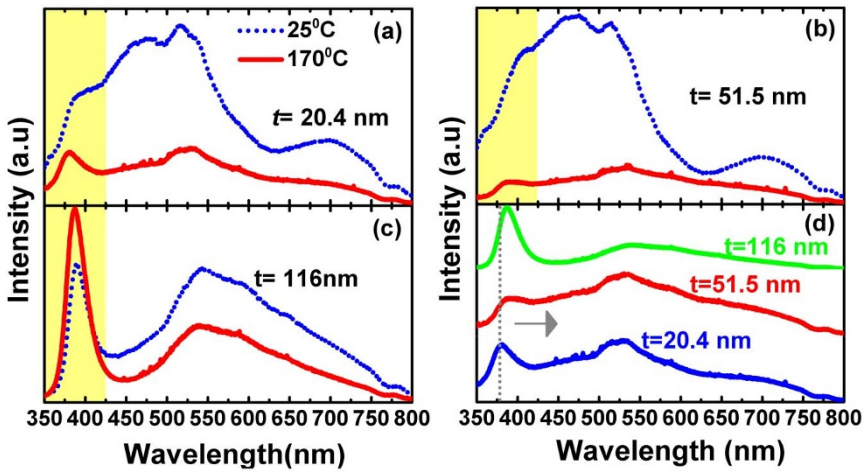

Figure 6 | Photoluminescence spectra of ZnO thin films of different thicknesses before and after annealing at 170°C. The yellow box indicates the free excitons emission zone. Arrow on (d) shows the shifting direction of the excitonic response with thickness of the films annealed at 170°C.

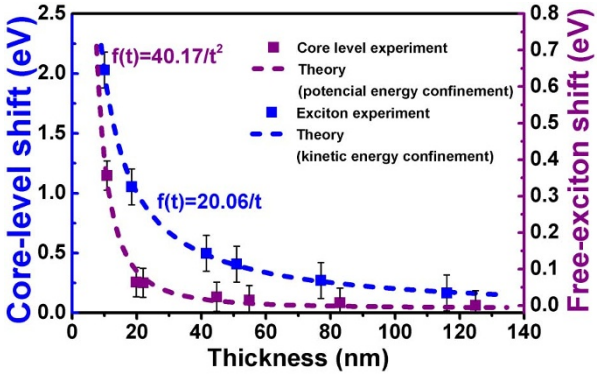

Figure 7 | Influence of the films thickness on core-electronic levels and free excitons energy in the ZnO films.

level shift, a thickness dependence of the type 1/t is obtained. Both, the evolution of the exciton energy as $1/t^2$ and of the core-level energy as 1/t, with t the confinement dimension, are well predicted by solving the Schrödinger's equation for the lowest excited electron-hole state[50]. The kinetic energy treated by the effective mass approximation gives a dependence of the type $1/t^2$. The 1/t dependence accounts for the potential energy evolution by solving of the high frequency dielectric function by atomic core electrons. The originality of the present study is to show the possibility to tune these energies by simply modifying the film thickness, i.e. the deposition time.

It has been reported that, when the nanoparticle size is close to the exciton Bohr radius, (2.87 nm), the exciton energy is around 5.5 eV, decreasing for nanoparticle sizes several times above ZnO Bohr radius. This phenomenon, named exciton confinement, has been observed in quantum dots[20,51] and nanocrystalline films[21]. If we extend this effect to the ZnO thin films, the free excitons are significantly confined for the films of thickness below 20 nm.

In conclusion, free exciton emission of ZnO thin films deposited by DC magnetron sputtering with varying thickness has been investigated. XRD spectra revealed that there is an improvement in crystal quality after annealing. The thickest films are made of close packed nanograins with grain sizes around 30 nm according to AFM results, which is in good agreement with the grain size obtained by XRD. But, due to the ZnO polar character, good crystallinity is not enough to produce the free exciton emission because the absorbed species, H_2O and OH on the surface of the as-deposited ZnO samples, suppress the free exciton emission.

XANES O-K edge spectra indicate that there is a difference in the band gap energy between the thinnest (t = 20.4 nm) and the other two ZnO films (t = 51.5 and 116.0 nm), and Zn 4d states are more predominant in the thickest films.

According to PL measurements, the annealing treatment enhances the signal of the free excitonic band due to removal of absorbed species. There is no evidence of H_2O and OH species after annealing according to XPS results. Therefore, the best ZnO thin film with high crystal quality and no adsorbed species was the film with $t = 116.0 \pm 0.8$ nm, showing a narrow and high intensity free exciton emission peak located at 3.20 eV, while for the thinnest film $t = 10.0 \pm 1.0$ nm, appeared a broad peak located at 3.56 eV. The exciton confinement related with the decrease in thickness was clearly observed, showing an inverse dependence on square of thickness, while the core-level electronic structure inversely depends on a first degree on the thickness.

Methods

Films preparation and characterization. Zinc oxide thin films of different thickness were synthesized onto glass substrates by DC reactive magnetron technique, using a pure metal target, in the presence of a argon/oxygen gas mixture. The flow rates were controlled with MKS flow-meters and the substrates were placed on a rotating substrate holder parallel to the zinc target with a separation distance of 50 mm. The working pressure was around 0.3 Pa and the target power was controlled with a MDX Advanced Energy power supply. The sample thickness was measured 25 times using a DEKTAK 150 STYLUS profilometer and, with the data collected, we calculated the standard deviation and average value. A similar procedure was used to calculate the roughness (Root- Mean-Square). After deposition, the samples were annealed in ambient atmosphere at 170°C and 250°C during 1 hour in a MELTA furnace. Finally, after the annealing treatment, the ZnO samples were stored in a vacuum chamber to avoid contamination.

Crystal structure characterization. X-ray diffraction (XRD) was employed to investigate the orientation of the ZnO films grown in this study. A BRUKER D8 X-ray diffractometer with Cu Kα radiation over an angle range of 2θ = 20–80° was used. The reported average grain size (*g*) in table I, was calculated using the Scherrer's formula[52]:

$$g = 0.94\lambda/\beta_{eff}\cos\theta \quad (1)$$

Where λ is the X-ray wavelength (0.15406 nm), θ is the Bragg diffraction angle, and β_{eff} is the effective FWHM of the (002) diffraction peak of ZnO, corrected for instrumental broadening[53].

Characterization of ZnO samples by X-ray photoelectron spectroscopy. The XPS investigation was carried out using a ESCALAB MK2 (VG) electron spectrometer with Al Kα X-ray monochromatic source (hv = 1486.6 eV). The C1s XPS peak (binding energy BE = 284.6 ev) was used as an internal reference line to accurately determine the position of other spectral lines. The spectra acquisition parameters (channel exposition, number of scans, analyzer parameters, etc) were selected in order to provide the optimal energy resolution and signal/noise ratio. The spectra were collected in "fresh" samples and after etching for up to 10 minutes by Ar^+ bombardment with a current of 20 mA. The etching ratio was 36 A/min and was quite enough to remove the C-O and C-H contamination in 10 minutes. The removal of contaminants has been controlled by measuring the decrease of the intensity of the C1s line on XPS spectra. All samples were cleaned under the same conditions until the C1s line was not detectable. During the tuning of the etching conditions, the Zn/O ratio was also measured. It was found that this value was constant during the whole cleaning procedure.

Morphological characterization of ZnO thin films. A NANOSCOPE IIIa atomic-force microscope in tapping mode was used. The image sizes obtained for all the films were from 1 mm × 1 mm to 14 mm × 14 mm; each image was composed of 512 × 512 pixels.

Characterization of the as-deposited ZnO thin films by X-ray absorption near-edge structure. XANES at the Zn-L3 and O-K edges was measured. The Total Electron Yield (TEY) and Total Fluorescence Yield (TFY) were collected with an energy step of 0.1 eV at the VESPERS Spherical Grating Monochromator (SGM) beamline located at the Canadian Light Source, Saskatoon, Canada.

Optical properties of the ZnO thin films. The transmittance spectra in the 250–800 nm wavelength region were measured in the ZnO films using a Varian Cary 500 UV-visible-NIR spectrophotometer, and for the photoluminescence (PL) measurements the samples were excited using 325 nm line of a 30 mW He-Cd laser. The PL signal was analyzed by a monochromator equipped with a 600 grooves/mm grating and by a photomultiplier tube cooled at 190 K. The transmittance and PL measurements were performed at room temperature.

1. Djuriic, A. B., Ng, A. M. C. & Chen, X. Y. ZnO nanostructures for optoelectronics: Material properties and device applications. *Progress in Quantum Electronics* **34**, 191–259.
2. Wang, Z. L. Novel nanostructures of ZnO for nanoscale photonics, optoelectronics, piezoelectricity, and sensing. *Applied Physics A: Materials Science and Processing* **88**, 7–15 (2007).
3. Qian, L., Zheng, Y., Xue, J. & Holloway, P. H. Stable and efficient quantum-dot light-emitting diodes based on solution-processed multilayer structures. *Nat Photon* **5**, 543–548 (2011).
4. Sandhu, A. The future of ultraviolet LEDs. *Nat Photon* **1**, 38–38 (2007).
5. Tsukazaki, A. *et al.* Repeated temperature modulation epitaxy for p-type doping and light-emitting diode based on ZnO. *Nat Mater* **4**, 42–46 (2005).
6. Monemar, B. Fundamental energy gap of gan from photoluminescence excitation spectra. *Physical Review B* **10**, 676–681 (1974).
7. Koch, S. W., Kira, M., Khitrova, G. & Gibbs, H. M. Semiconductor excitons in new light. *Nat Mater* **5**, 523–531 (2006).
8. Liao, Z.-M. *et al.* Strain induced exciton fine-structure splitting and shift in bent ZnO microwires. *Sci. Rep.* **2** (2012).
9. Johnston, K. *et al.* Identification of donor-related impurities in ZnO using photoluminescence and radiotracer techniques. *Physical Review B* **73**, 165–212 (2006).
10. Scholes, G. D. & Rumbles, G. Excitons in nanoscale systems. *Nat Mater* **5**, 683–696 (2006).

11. Zimmler, M. A., Voss, T., Ronning, C. & Capasso, F. Exciton-related electroluminescence from ZnO nanowire light-emitting diodes. *Applied Physics Letters* **94** (2009).
12. Choi, Y. S., Kang, J. W., Hwang, D. K. & Park, S. J. Recent advances in ZnO-based light-emitting diodes. *IEEE Transactions on Electron Devices* **57**, 26–41.
13. Schaller, R. D., Agranovich, V. M. & Klimov, V. I. High-efficiency carrier multiplication through direct photogeneration of multi-excitons via virtual single-exciton states. *Nat Phys* **1**, 189–194 (2005).
14. Klimov, V. I. *et al.* Optical gain and stimulated emission in nanocrystal quantum dots. *Science* **290**, 314–317 (2000).
15. Krauss, T. D. Laser technology: Less excitement for more gain. *Nature* **447**, 385–386 (2007).
16. Safi, I. Recent aspects concerning DC reactive magnetron sputtering of thin films: A review. *Surface and Coatings Technology* **127**, 203–219 (2000).
17. Musil, J., Baroch, P., VlÄ ek, J., Nam, K. H. & Han, J. G. Reactive magnetron sputtering of thin films: Present status and trends. *Thin Solid Films* **475**, 208–218 (2005).
18. Zhao, H., Xiong, W. & Zhu, M. Z. Exciton in ZnO film. *International Journal of Modern Physics B* **21**, 5237–5245 (2007).
19. Cheng, H. M., Lin, K. F., Hsu, H. C. & Hsieh, W. F. Size dependence of photoluminescence and resonant Raman scattering from ZnO quantum dots. *Applied Physics Letters* **88** (2006).
20. Dallali, L., Jaziri, S., El Haskouri, J. & Amorós, P. Optical properties of exciton confinement in spherical ZnO quantum dots embedded in SiO_2 matrix. *Superlattices and Microstructures* **46**, 907–916 (2009).
21. Nie, J. C. *et al.* Quantum confinement effect in ZnO thin films grown by pulsed laser deposition. *Applied Physics Letters* **93** (2008).
22. Kovalev, A. I., Wainstein, D. L., Rashkovskiy, A. Y., Osherov, A. & Golan, Y. Size shift of XPS lines observed from PbS nanocrystals. *Surface and Interface Analysis* **42**, 850–854 (2010).
23. Bordass, W. T. & Linnett, J. W. PHOTOELECTRON SPECTROSCOPY AND ADSORBED SPECIES. *Nature* **222**, 660–661 (1969).
24. Chen, M. *et al.* X-ray photoelectron spectroscopy and auger electron spectroscopy studies of Al-doped ZnO films. *Applied Surface Science* **158**, 134–140 (2000).
25. Henke, L., Nagy, N. & Krull, U. J. An AFM determination of the effects on surface roughness caused by cleaning of fused silica and glass substrates in the process of optical biosensor preparation. *Biosensors and Bioelectronics* **17**, 547–555 (2002).
26. Horwat, D. *et al.* On the deactivation of the dopant and electronic structure in reactively sputtered transparent Al-doped ZnO thin films. *Journal of Physics D: Applied. Physics.* **43**, 1–4 (2010).
27. Mϕller, P. J., Komolov, S. A. & Lazneva, E. F. A total current spectroscopy study of metal oxide surfaces: I. Unoccupied electronic states of ZnO and MgO. *Journal of Physics Condensed Matter* **11**, 9581–9588 (1999).
28. Jullien, M. *et al.* Influence of the nanoscale structural features on the properties and electronic structure of Al-doped ZnO thin films: An X-ray absorption study. *Solar Energy Materials and Solar Cells* **95**, 2341–2346 (2011).
29. Claeyssens, F. *et al.* Growth of ZnO thin films - Experiment and theory. *Journal of Materials Chemistry* **15**, 139–148 (2005).
30. Uedono, A. *et al.* Defects in ZnO thin films grown on $ScAlMgO_4$ substrates probed by a monoenergetic positron beam. *Journal of Applied Physics* **93**, 2481–2485 (2003).
31. Holmes-Siedle, A. G. Defects in oxides. *Nature* **250**, 689–690 (1974).
32. Burstein, E. Anomalous Optical Absorption Limit in InSb. *Physical Review* **93**, 632–633 (1954).
33. Sans, J. A., Sánchez-Royo, J. F., Segura, A., Tobias, G. & Canadell, E. Chemical effects on the optical band-gap of heavily doped ZnO: MIII (M = Al,Ga,In): An investigation by means of photoelectron spectroscopy, optical measurements under pressure, and band structure calculations. *Physical Review B - Condensed Matter and Materials Physics* **79** (2009).
34. Banerjee, P., Lee, W. J., Bae, K. R., Lee, S. B. & Rubloff, G. W. Structural, electrical, and optical properties of atomic layer deposition Al-doped ZnO films. *Journal of Applied Physics* **108**.
35. Jia, J., Takasaki, A., Oka, N. & Shigesato, Y. Experimental observation on the Fermi level shift in polycrystalline Al-doped ZnO films. *Journal of Applied Physics* **112**.
36. Cho, S. *et al.* Photoluminescence and ultraviolet lasing of polycrystalline ZnO thin films prepared by the oxidation of the metallic Zn. *Applied Physics Letters* **75**, 2761–2763 (1999).
37. Wang, Y. G. *et al.* Photoluminescence study of ZnO films prepared by thermal oxidation of Zn metallic films in air. *Journal of Applied Physics* **94**, 354–358 (2003).
38. Maniv, S., Westwood, W. D. & Colombini, E. Pressure and angle of incidence effects in reactive planar magnetron sputtered ZnO layers. *Journal of vacuum science & technology* **20**, 162–170 (1982).
39. Daniel, G. P. *et al.* Effect of annealing temperature on the structural and optical properties of ZnO thin films prepared by RF magnetron sputtering. *Physica B: Condensed Matter* **405**, 1782–1786 (2010).
40. Wang, Y. *et al.* Determination of the polarity of ZnO thin films by electron energy-loss spectroscopy. *Physics Letters, Section A: General, Atomic and Solid State Physics* **320**, 322–326 (2004).
41. Allen, M. W. *et al.* Polarity effects in the x-ray photoemission of ZnO and other wurtzite semiconductors. *Applied Physics Letters* **98**, 16–18 (2011).
42. Taylor, H. S. Activated adsorption of hydrogen by zinc and chromium oxides. *Nature* **128**, 636–636 (1931).
43. Lal, R. B. & Arnett, G. M. Effect of Ultra-violet Irradiation on the Electrical Conductivity of Zinc Oxide Single Crystals. *Nature* **208**, 1305–1305 (1965).
44. Reynolds, D. C., Look, D. C., Jogai, B. & Morkoç, H. Similarities in the bandedge and deep-centre photoluminescence mechanisms of ZnO and GaN. *Solid State Communications* **101**, 643–646 (1997).
45. Vanheusden, K. *et al.* Mechanisms behind green photoluminescence in ZnO phosphor powders. *Journal of Applied Physics* **79**, 7983–7990 (1996).
46. Bylander, E. G. Surface effects on the low-energy cathodoluminescence of zinc oxide. *Journal of Applied Physics* **49**, 1188–1195 (1978).
47. Cao, W. & Du, W. Strong exciton emission from ZnO microcrystal formed by continuous 532 nm laser irradiation. *Journal of Luminescence* **124**, 260–264 (2007).
48. Qian, L., Zheng, Y., Xue, J. G. & Holloway, P. H. Stable and efficient quantum-dot light-emitting diodes based on solution-processed multilayer structures. *Nature Photonics* **5**, 543–548 (2011).
49. Zhou, H. *et al.* Effect of the (OH) surface capping on ZnO quantum dots. *Physica Status Solidi (B) Basic Research* **229**, 825–828 (2002).
50. Brus, L. E. Electron-electron and electron-hole interactions in small semiconductor crystallites: The size dependence of the lowest excited electronic state. *The Journal of Chemical Physics* **80**, 4403–4409 (1984).
51. Dang, C. *et al.* Red, green and blue lasing enabled by single-exciton gain in colloidal quantum dot films. *Nature Nanotechnology* **7**, 335–339 (2012).
52. Holzwarth, U. & Gibson, N. The Scherrer equation versus the 'Debye-Scherrer equation'. *Nature Nanotechnology* **6**, 534–534 (2011).
53. Van Dover, R. B., Lang, D. V., Green, M. L. & Manchanda, L. Crystallization kinetics in amorphous $(Zr_{0.62}Al_{0.38})O_{1.8}$ thin films. *Journal of Vacuum Science and Technology, Part A: Vacuum, Surfaces and Films* **19**, 2779–2784 (2001).

Acknowledgments

This work was supported by the Spanish Ministry of Science and Innovation through the FUNCOAT project, within the program Consolider Ingenio (ref. CSD2008-00023). A. Rashkovskiy was partially supported by Russian Federation Scholarship #2040.2012.1. The authors are also indebted to L. Vázquez by his valuable contribution in the AFM analysis.

Author contributions

A. M. wrote the article and analyzed the experimental data. The experimental work was performed by A.M., D.H., P.M., A.R., and D.W. All the authors participated equally in the discussion, and the article was reviewed by A.K., D.H., J.M.A. and J.L.E.

Additional information

Supplementary information accompanies this paper at http://www.nature.com/scientificreports

Competing financial interests: The authors declare no competing financial interests.

How to cite this article: Mosquera, A.A. *et al.* Exciton and core-level electron confinement effects in transparent ZnO thin films. *Sci. Rep.* **3**, 1714; DOI:10.1038/srep01714 (2013).

SCIENTIFIC REPORTS

Corrigendum: Exciton and core-level electron confinement effects in transparent ZnO thin films

Adolfo A. Mosquera, David Horwat, Alexandr Rashkovskiy, Anatoly Kovalev, Patrice Miska, Dmitry Wainstein, Jose M. Albella & Jose L. Endrino

Scientific Reports **3**:1714; doi: 10.1038/srep01714; published online 24 April 2013; updated on 31 July 2015

This Article contains errors in Figure 7: the colour legends have been inverted and there is an offset in the x-axis for the 'Theory (kinetic energy confinement)' curve. The correct Figure 7 appears below as Figure 1.

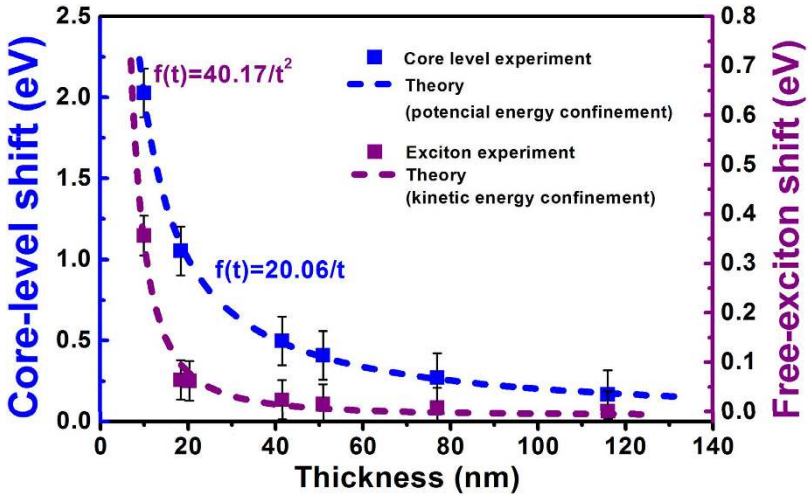

Figure 1.